

## Geology and geochemistry of granitic rocks and their surrounding stream sediments at Gabal Rei El-Garrah area, Central Eastern Desert, Egypt

El Mezayen, A. M<sup>1</sup>., Abdel Ghani, I. M<sup>2</sup>., El Balakssy, S. S<sup>2</sup>. and El Setouhy, M. S<sup>2</sup>.

<sup>1</sup>Geology Department, Faculty of Science, Al Azhar University Egypt.

<sup>2</sup>Nuclear Materials Authority, P. O. Box 530 El Maadi, Cario, Egypt.

[mostafa24264@hotmail.com](mailto:mostafa24264@hotmail.com)

**Abstract:** Gabal Rei El-Garrah area lies in the Central Eastern Desert of Egypt. The rock types in the study area comprise metavolcanics, older granitoids, younger gabbros, monzogranites, quartz-feldspar porphyry dykes and syenogranites. Beyond the extreme western part of the study area, these Precambrian basement rocks are unconformably capped with Nubian Sandstones. The basement rock units of Rei El-Garrah area are dissected by several Wadis. The main wadis are Wadi Rei El-Garrah, Wadi El-Missikat, Wadi El-Markh and Wadi El-Gidami. The geochemical analyses of the examined older granitoids and younger granites exhibit that the studied monzogranites and syenogranites have higher silica, total alkalis content and lower Al<sub>2</sub>O<sub>3</sub>, FeO<sup>t</sup> and CaO than older granitoids. SiO<sub>2</sub> and D.I. variations with the major oxides and trace elements indicate that a compositional gap exists between the plots of the older granitoids on one hand and those for younger granites on the other hand suggesting discontinuous or rather independent processes of magma evolution. The older granitoids and younger granites are peraluminous due to high alumina contents. The older granitoids belong to a calc-alkaline suite with mild tholeiitic tendency evolved in a volcanic arc while the younger granites are calc-alkaline due to the high total alkali contents and low MgO and FeO<sup>t</sup> contents and originated in within-plate environment. The studied stream sediments show extraordinary anomalous contents from Pb, Zr, Rb and Zn in correlation with the other trace elements. Wadi El-Missikat contains the highest contents of Pb, Rb and Ga correlating to the other Wadis which are mainly related to the presence of cotunnite (PbCl<sub>2</sub>) and other silicate minerals mainly originated from the surrounding granitic rocks. The area around Rei El Garrah contains the highest contents of Zr, Zn and Y in relation to other Wadis resulting from the presence of zircon and other silicate minerals. However, Wadi El Markh has the highest contents of Cr, Ni, Zn and V with respect to other Wadis which are mainly originated from the surrounding mafic-ultramafic rocks.

[El Mezayen, A. M., Abdel Ghani, I. M., El Balakssy, S. S. and El Setouhy, M. S. **Geology and geochemistry of granitic rocks and their surrounding stream sediments at Gabal Rei El-Garrah area, Central Eastern Desert, Egypt.** *J Am Sci* 2017;13(11):17-37]. ISSN 1545-1003 (print); ISSN 2375-7264 (online). <http://www.jofamericanscience.org>. 3. doi:10.7537/marsjas131117.03.

**Key words:** Geology and geochemistry, Granitic Rocks, Gabal Rei El-Garrah area and Eastern Desert of Egypt.

### 1. Introduction

The Arabian-Nubian-Shield is composed of a number of island-arc terrains together with fragments of oceanic lithosphere and minor continental terrains (*Abdeen and Greiling, 2005*). This structural sequence is intruded by syn- to post- tectonic granites. The Egyptian Eastern Desert lies in the Nubian part of the Arabian-Nubian-Shield and it forms a discontinuous range of mountain groups, more or less coherently disposed in linear direction roughly parallel to the Red Sea coast and is geologically similar to crustal block of the western part of the Arabian Peninsula. Geological studies indicate that Arabian-Nubian-Shield rocks are formed through a variety of tectonic regimes. The Nubian segment of the Arabian-Nubian-Shield has been evolved between 1100 and 500 Ma from an oceanic and volcanic arc environment to a stable craton (*El Shazly et al., 1981*).

Three distinct basement domains could be recognized within the Eastern Desert; a) the northern Eastern Desert (NED), b) central Eastern Desert

(CED), and c) southern Eastern Desert (SED) (*El Ramly, 1972; Stern and Hedge, 1985*).

The post-tectonic younger granites represent the last major magmatic event recognized in crystalline basement of Egypt; they belong to the Pan-African plutonism within a narrow time span between 550 and 600 Ma (*Greenberg, 1981*). These granites especially their late more siliceous phases, are characterized by high radioactivity (*Hussein and El Kassas, 1980*).

The study area is a part of the Central Eastern Desert of Egypt. It covers about 163,53 km<sup>2</sup> of crystalline basement rocks at midpoint between the Nile Valley and the Red Sea Coast, along the Qena-Safaga main road and it is bounded between latitudes 26° 23' 30" and 26° 31' 30" N and longitudes 33° 21' 30" and 33° 26' 40" E (*Fig. 1*). The present study aims to shed the lights on the geological and geochemical characteristics of the syn- and post-tectonic granites and stream sediments of the investigated area.

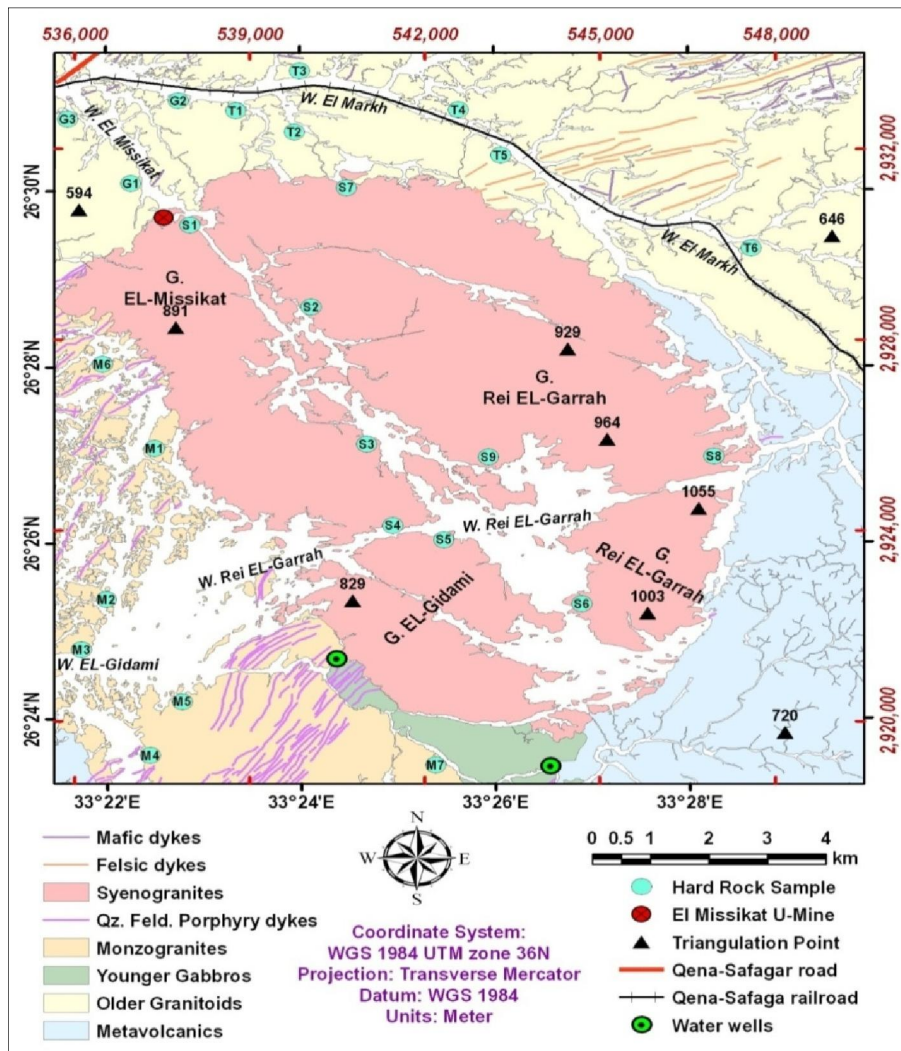


**Fig. 1:** Geological and sample location map of granitic rocks of Gabal Rei El-Garrah area, Central Eastern Desert, Egypt.



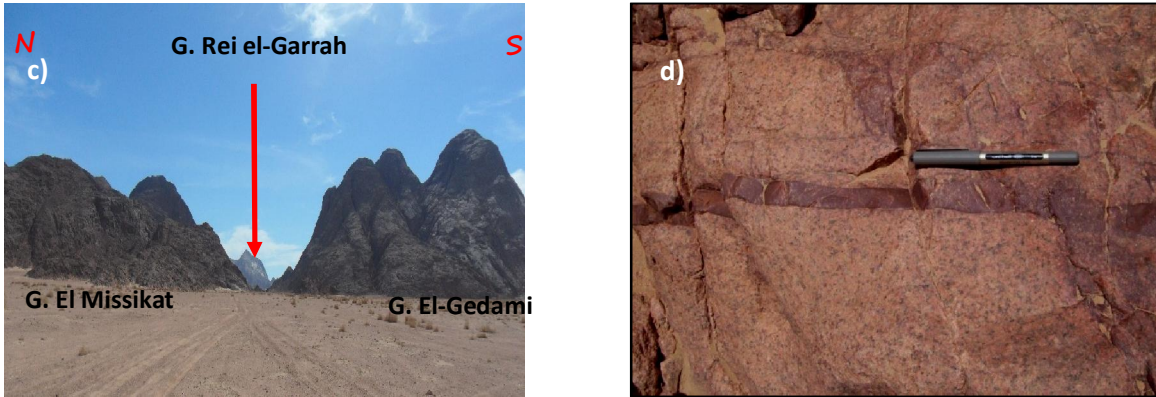


Fig. 2.a: Offshoots of syenogranites intruding metavolcanics, W. Rei El-Garrah.  
 Fig. 2.b: Syenogranite offshoots in tonalite, north east G. Rei EL-Garrah.  
 Fig. 2.c: General view showing the three main plutons of the younger granites in the study area  
 Fig.2.d: Jasper veinlet in hematitized syenogranites, G. El-Missikat

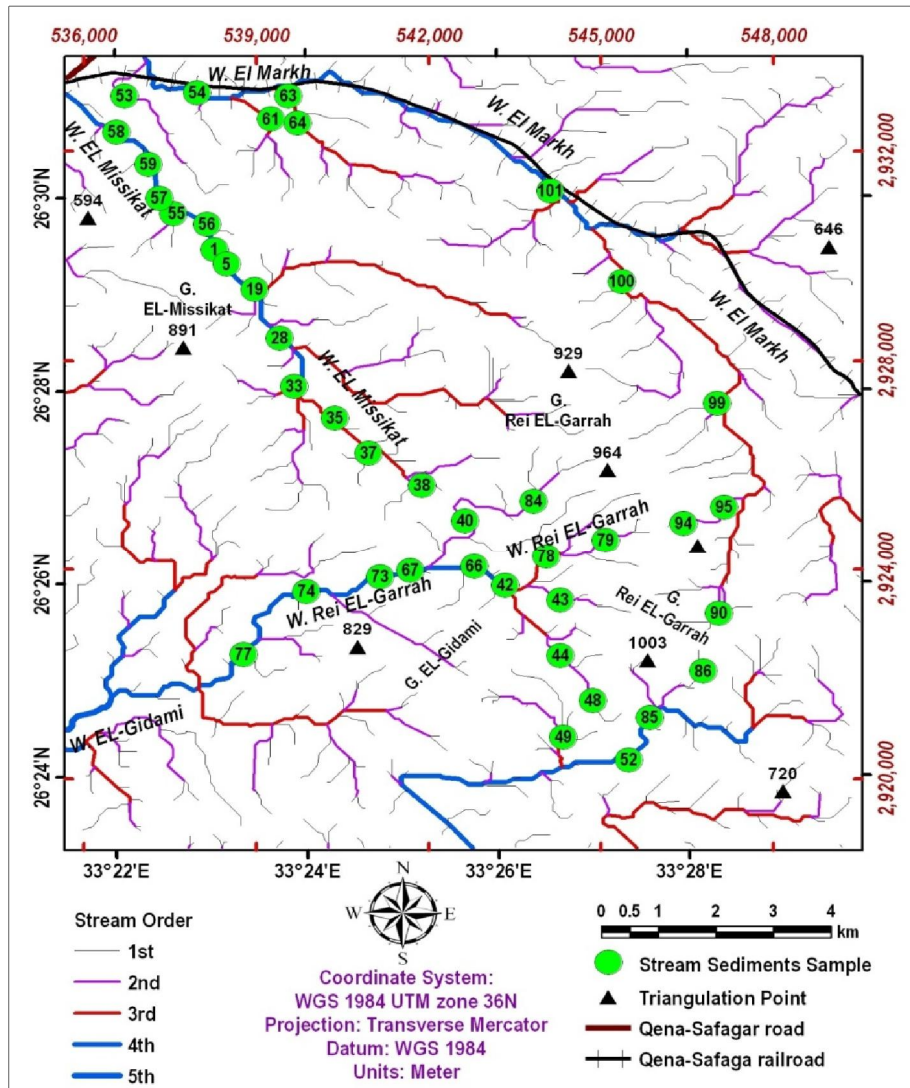
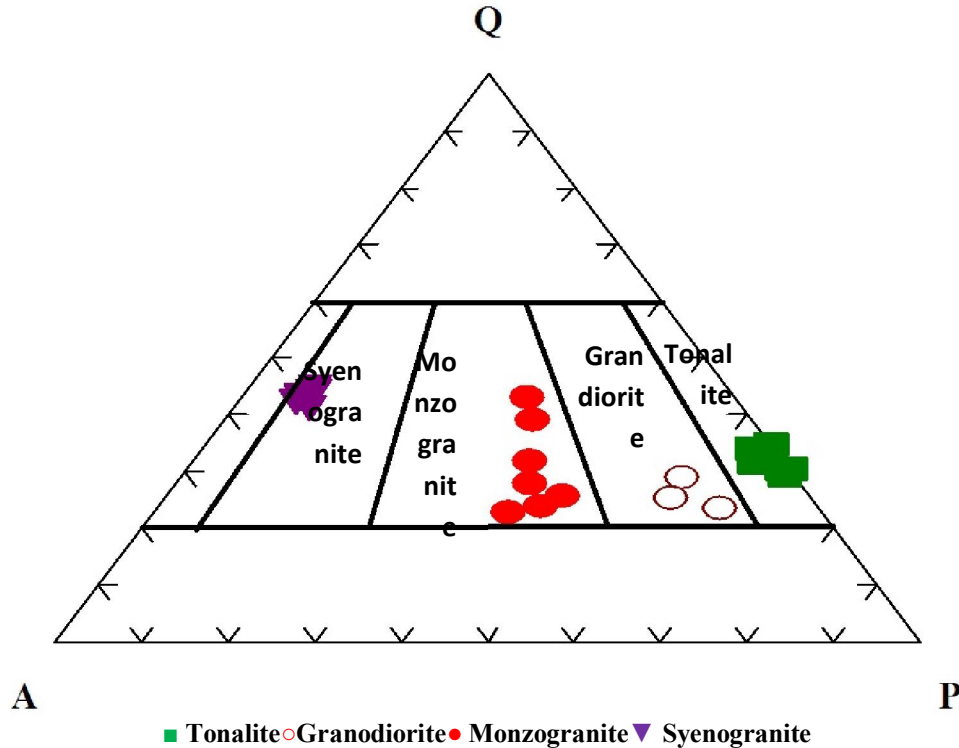


Fig. 3: Sample location map of stream sediments of Gabal Rei El-Garrah area, Central Eastern Desert, Egypt.



**Fig. 4: Classification of the El-Garrah granitic rocks using modal analyses of (Streckeisen, 1976a). Where Q=Quartz, A=Alkali feldspar and P=plagioclase**

## 2. Geologic Setting

Gabal Rei El-Garrah area lies in the CED of Egypt south Qena-Safaga road just east the western boundary between the basement rocks and the sedimentary cover. Based on field relations and observations, the rock types in the study area comprise metavolcanics, older granitoids, younger gabbros, monzogranites, quartz-feldspar porphyry dykes and syenogranites. Beyond the extreme western part of the study area, these Precambrian basement rocks are unconformably capped with Nubian Sandstones.

**The Metavolcanics** represent the oldest rock unit in the study area and are represented by metabasalts and meta-andesites alternating with their pyroclastics. They are highly metamorphosed up to amphibolite facies near the contact with younger granites especially at the eastern and southern borders of G. Rei El-Garrah granitic masses. Several irregular offshoots of different sizes extend from syenogranites into metavolcanics (**Fig. 2.a**). In addition, they may be found as xenoliths in the older granitoids and the first phase of younger granites (monzogranites).

**Older granitoids** are represented by gneissose quartz-diorites and granodiorites. Generally, the two varieties of older granitoids crop out together along the northern parts of the study area and intruded by the younger granites exhibiting sharp intrusive contacts. Older granitoids are characterized by whitish

grey to dark grey colors but sometimes become darker when contain xenoliths and roof-pendants of the older metavolcanics. The color of the older granitoids may turn into pink due to the presence of several offshoots of younger granites as in W. El Markh) (**Fig. 2.b**). The older granitoids show a clear heterogeneous nature and gradational contacts with all the surrounding rocks.

**Younger gabbros** found as elongated mass extending along the southern periphery of G. El-Gidami. They intrude and carry roof-pendants of the metavolcanics and in turn they are intruded by the younger granites.

**The younger granites** are mainly represented by three plutons namely G. El-Missikat, G. Rei El-Garrah, G. El-Gidami (**Fig. 2.c**) and scattered granitic masses with low to moderate topography west of Gabal El Missikat and West of G. El-Gidami. Two varieties of younger granites are identified; monzogranites and syenogranites. Field relationships and observations suggest that the younger granites in the study area were intruded in successive pulses, starting with the greyish pink granites (monzogranites), which are intruded by the pink granites (syenogranites). These granites in general, are characterized by their massive nature and sharp intrusive contacts with all surrounding rocks. Alteration processes are local and restricted along fractures, fault planes and shear zones. These

alteration processes are represented by silicification, hematization and kaolinization. Several zoned and unzoned oval-shaped and/or elongated pegmatite pockets and veins are also encountered in syenogranites (**Fig. 2.d**). They are mainly composed of quartz and K-feldspars with little mica, green to violet fluorite and jasper. Both of the granitic rocks and the country rocks are dissected by several dykes of different compositions and attitudes. They are mainly having the NE-SW, E-W, N-S and NW-SE directions. They vary in width from few centimetres up to 8 metres and lengths from 150 metres up to several kilometres (about 8 km). Dykes are generally represented by quartz-feldspar porphyry dykes, felsic and mafic dykes.

**Stream Sediments** The basement rock units of Rei El-Garrah area, exhibiting high, moderate and low relief, are dissected by several Wadis. The main wadis are Wadi Rei El-Garrah, Wadi El-Missikat, Wadi El-Markh and Wadi El-Gidami. The direction of these wadis are coincident with the large scale faults and covered mainly by stream sediments. The thickness of the stream sediments of the studied area can be estimated from the groundwater wells. It ranges from 25 to 30 meters. They are composed mainly of loose sand with gravels, pebbles and rarely cobbles, which embedded in this sandy matrix. The samples were collected at interval of about 0.5 km, the average weight of each sample is about 7kg including different sizes. Twenty five rock samples and forty-one stream sediment samples are collected for geological and geochemical investigations for granitic rocks and stream sediments of the study area (**Fig.1 & Fig.3**).

**Petrography** Granitic rocks are the largely dominant rock unit displayed in the study area. So, they should be studied in detail petrographically. The modal analyses that calculated for the studied rocks classified them to two main rock clans the first is older granitoids and the second is younger granites (**Fig.4**).

### 3.1. Older Granitoids

The older granitoids of the studied area are mainly composed mainly of plagioclase associated with quartz and mafic minerals, while the potash feldspars are nearly absent in the tonalite variety and present in appreciable amount in the granodiorite variety.

#### Tonalite

Tonalite of Rei El-Garrah is gray-colored rock characterized by medium grain size (4mm length) and holocrystalline equigranular texture. Plagioclase is the main feldspar minerals occurring as euhedral crystals of andesine ( $An_{42}$ ). They are characterized by zonation and lamellar twinning (**Fig. 5.a**); most of the crystals are slightly saussuritized. Potash feldspars are nearly absent except rare crystals of perthite. Quartz occurs as anhedral crystal mostly elongated exhibiting its

characteristic wavy extinction. Mafic minerals are relatively abundant and they are mainly hornblende which occur as foliated crystals or as well-formed basal crystals exhibiting its characteristic two-sets cleavage. The accessory minerals are rare and mainly represented by zircon and epidote.

#### Granodiorite

The studied granodiorite is composed mainly of plagioclase, potash feldspars, quartz and mafic minerals. Plagioclase is the main feldspar mineral and occurs as euhedral crystals of andesine ( $An_{36}$ ) characterized by lamellar twinning and occasionally zoned. Potash feldspars are less common present as medium crystals of patchy perthite and string types enclosing finer crystals of orthoclase and albite. Quartz mostly found as elongated grains characterized by undulose extinction. Mafic minerals are represented mainly by biotite and hornblende which are strongly pleochroic from yellow, green to dark green characterized by simple twinning (**Fig. 5.b**). Accessory minerals are mainly zircon, allanite, apatite and titanite.

### 3.2. Young granites

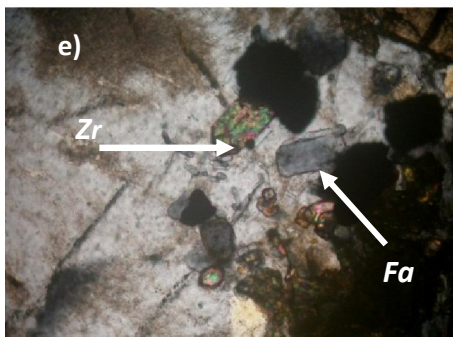
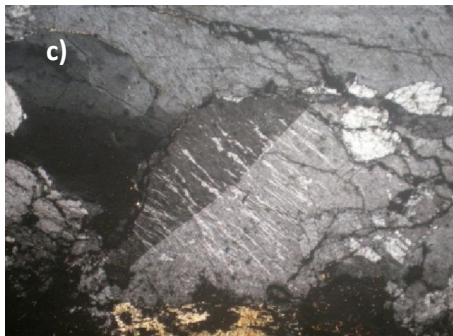
Petrographic studies and modal analyses of the studied younger granites indicated that, these rocks are subsolvus granites composed of two-feldspars (plagioclase and potash feldspar). They can be classified, according to the percentages of plagioclase, potash feldspars and quartz, to two granitic varieties (monzogranites and syenogranites).

Megascopically, **Monzogranites** are coarse-grained, characterized by pinkish white color. Under the microscope, they are composed essentially of plagioclase, potash feldspars, quartz, biotite and hornblende. Potash feldspar occurs as subhedral crystals of orthoclase perthite (**Fig. 5.c**). Plagioclase ( $An_{14}$ ) found as subhedral to euhedral prismatic crystals of oligoclase and showing its characteristic lamellar twinning. Some crystals of plagioclase are partially saussuritized (**Fig. 5.d**). Quartz occurs as anhedral crystals associating the other constituents or as skeletal crystals associating the perthite or plagioclase. Mafic minerals present as biotite and hornblende. Biotite is more common occurring as flakes enriched by iron oxides and transformed to ferribiotite (annite), It encloses fractured crystals of metamict zircon. Some biotite crystals are partially chloritized to penninite. Muscovite is rare and presents as secondary minute flake enclosed in the plagioclase. Zircon, fluorapatite and titanite are the main accessory minerals. Zircon is included in biotite as minute crystals surrounded by pleochroic halos. It also occurs as well formed crystals exhibiting its characteristic interference colors associating fluorapatite and opaque minerals (**Fig. 5.e**) or associating titanite and opaques.

#### Syenogranite:

Syenogranites of Rei El-Garrah area are medium to coarse-grained, leucocratic and pale pink to faint brownish pink in color. Microscopic investigation clarified that, this rock is composed essentially of potash feldspar, plagioclase, quartz and biotite. It is characterized by porphyritic and graphic textures. Potash feldspar present as phenocrysts of string perthite surrounded by groundmass of quartz, perthite and plagioclase forming glomeroporphyritic texture. They are also graphically intergrown with quartz forming graphic texture (**Fig. 5.f**). Plagioclase ( $An_8$ ) occurs as phenocrysts associating the potash feldspars or as fine crystals (1.5 mm) in the

groundmass. They are subhedral to euhedral crystals showing albite twinning, zonation. Quartz is found as anhedral to subhedral crystals varying in size from fine- to medium-grained. Biotite represents the main mafic minerals; it is found as irregular flakes, brown in color and displays strong pleochroism. Zircon is the main accessory mineral occurring as small prismatic crystals in biotite. Monazite occurs in aggregates of minute crystals included in chlorite (**Fig. 5.g**). Allanite occurs as well- formed crystals enriched with iron oxides, characterized by masked interference colors (**Fig. 5.h**) and occasionally exhibits well developed zonation.



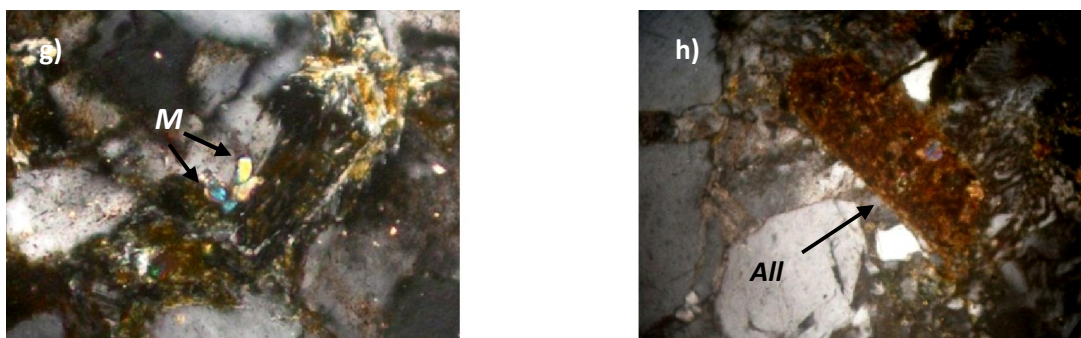


Fig. 5.a: Photomicrograph of zoned crystals of plagioclase partially saussuritized, CN. X10, tonalite.

Fig. 5.b: Photomicrograph showing a crystal of hornblende with simple twinning, CN. X10, granodiorite.

Fig. 5.c: Photomicrograph showing Subhedral crystal of orthoclase perthite, CN. X5, monzogranite.

Fig. 5.d: Photomicrograph showing partially saussuritized plagioclase, CN. X10, monzogranite

Fig. 5.e: Photomicrograph showing Euhedral crystal of zircon (Zr) associating fluorapatite (Fa) included in plagioclase CN X20, monzogranite.

Fig. 5.f: Photomicrograph showing Potash feldspar and quartz showing micro graphic texture CN. X10, Syenogranite.

Fig. 5.g: Photomicrograph showing Aggregate of monazite (M) crystals associated chlorite CN. X40, Syenogranite.

Fig. 5.h: Photomicrograph showing Well-formed crystal of allanite (All) enriched with iron oxides. CN. X20, Syenogranite.

## Geochemistry

### Materials and Methods

The chemical analyses of twenty-five samples representative samples exposed in the studied area were chemically analysed and listed in (Table 1, 3 and 5). These include (9) samples from syenogranite, (7) samples from monzogranite, (6) samples from tonalite and (3) samples from granodiorite. Major oxides were carried out according to the conventional wet chemical techniques of (Shapiro and Brannock, 1962) with some modification given by (El Reedy, 1984) and some trace elements concentrations were carried out by using XRF technique (Phillips XRF spectrometer, model X' Unique II, PW 1510 with automatic sample changer. The calculated CIPW normative compositions of the analyzed samples are listed also in (Table 2, 4, 6).

### General Geochemical characteristics:

#### 4.1. Harker diagrams

The variations between  $\text{SiO}_2$  and the major oxides indicate that, there is a negative correlation between with  $\text{Al}_2\text{O}_3$ ,  $\text{FeO}$ ,  $\text{Fe}_2\text{O}_3$  and  $\text{MgO}$  (where these oxides decrease with increasing  $\text{SiO}_2$ ). It is obvious from (Fig. 6), that a compositional gap exists between the plots of the older granitoids on one hand and those for younger granites on the other hand. This suggests discontinuous or rather independent processes of magma evolution i.e. these rocks are not cogenetic. The overlap exists between the plots of each of the monzogranites and the syenogranites suggests that they are cogenetic.

The distribution and variation of some trace elements during igneous processes can be shown by plotting their contents against  $\text{SiO}_2$ . The Rb, Zr and Y exhibit an increasing trend with the increasing in  $\text{SiO}_2$  (positive correlation) from tonalite to syenogranites. The Sr show a decreasing trend from tonalite to syenogranites (negative correlation).

Table 1: Chemical composition of the investigated older granitoids

Rock type	Granodiorites			Tonalites					
S. No.	G1	G2	G3	T1	T2	T3	T4	T5	T6
<b>Major Oxides (wt. %)</b>									
$\text{SiO}_2$	67.5	67.8	68.1	60.01	61.93	61.52	63.05	63.47	62.95
$\text{TiO}_2$	0.51	0.45	0.61	0.71	0.63	0.77	0.66	0.73	0.69
$\text{Al}_2\text{O}_3$	14	14.5	13.6	16.42	15.89	16.32	16	15.5	15.97
$\text{Fe}_2\text{O}_3$	1.87	1.7	1.9	4.2	4.12	4.05	3.87	3.5	3.56
$\text{FeO}$	1.65	1.55	1.4	3.52	3.22	3.25	3.2	3.34	3.13
$\text{MnO}$	0.01	0.03	0.02	0.04	0.03	0.01	0.04	0.02	0.03
$\text{MgO}$	1.1	0.87	0.9	2.61	2.43	2.35	1.67	1.62	2.18
$\text{CaO}$	4.54	4.7	4.71	4.43	3.16	4.23	3.47	3.66	3.67

Rock type	Granodiorites			Tonalites					
S. No.	G1	G2	G3	T1	T2	T3	T4	T5	T6
Na <sub>2</sub> O	4.2	4.22	4.1	4.75	4.63	4.24	4.56	4.43	4.41
K <sub>2</sub> O	2.5	2.27	2.3	1.51	1.38	1.42	1.31	1.45	1.44
P <sub>2</sub> O <sub>5</sub>	0.1	0.08	0.07	0.21	0.03	0.02	0.1	0.12	0.07
L.O.I	2.02	1.81	2.2	1.56	2.3	1.72	1.9	1.85	1.8
Total	100	99.98	99.91	99.97	99.75	99.9	99.83	99.69	99.9
Trace elements (ppm)									
Sr	491	520	497	150	133	140	123	137	145
Ga	28	22	25	17	15	14	13	15	12
Ba	688	695	700	180	207	175	192	177	199
Rb	59	64	70	25	14	17	12	23	15
Zr	73	65	68	70	63	65	72	61	59
Nb	14	10	12	6	5	3	2	4	5
Cr	17	15	14	10	14	13	11	8	11
Ni	12	9	11	3	4	3	2	4	3
V	30	32	35	27	35	44	31	25	40
Zn	49	53	62	33	22	18	15	12	14
Cu	7	6	5	8	5	12	7	4	9
Pb	13	15	12	2	4	3	3	4	3
Y	19	21	18	19	22	18	17	23	26

Table 2: CIPW-norm and geochemical parameters of the investigated older granitoids

Rock type	Granodiorite			Tonalite					
S. No.	G1	G2	G3	T1	T2	T3	T4	T5	T6
CIPW normative minerals									
Qz	24.78	25.49	27.22	13.51	19.22	18.64	21.56	21.76	20.48
Or	15.09	13.68	13.92	9.08	8.38	8.55	7.91	8.77	8.68
Ab	36.23	36.33	35.46	40.79	40.15	36.5	39.35	38.27	37.99
An	12.18	14.14	12.16	19.3	15.92	21.27	16.99	17.85	18.15
Di	7.33	6.23	5.03	1.43	-	-	-	-	-
Hy	-	-	-	7.87	7.79	5.96	5.96	6.25	7.31
Wo	0.42	0.57	2.04	-	-	-	-	-	-
Cor	-	-	-	-	1.11	0.99	0.99	0.24	0.63
MA	2.77	2.51	2.82	6.19	6.13	5.73	5.73	5.19	5.26
HM	-	-	-	-	-	-	-	-	-
ILM	0.99	0.87	1.19	1.37	1.23	1.28	1.28	1.42	1.34
Rut	-	-	-	-	-	-	-	-	-
Ap	0.22	0.18	0.16	0.47	0.07	0.22	0.22	0.27	0.16
Geochemical parameters									
C.I.	19.5	20.37	17.19	26.24	21.37	21.16	21.16	22.23	23.27
AGP.I.	0.69	0.65	0.68	0.58	0.57	0.56	0.56	0.57	0.55
D.I.	76.1	75.5	76.61	63.38	67.75	63.7	68.83	68.79	67.16
M.I.	76.19	78.88	78.57	74.73	75.13	75.65	80.89	80.85	75.42
F.I.	59.61	58	57.61	58.56	65.54	57.23	62.85	61.64	61.45

**Table 3: Chemical composition of the investigated younger granites (monzogranites)**

Rock type	Monzogranites						
S. No.	M1	M2	M3	M4	M5	M6	M7
<b>Major Oxides (wt. %)</b>							
SiO <sub>2</sub>	73	71.9	72.5	72.3	72.66	72.4	72.6
TiO <sub>2</sub>	0.7	0.5	0.35	0.42	0.46	0.5	0.31
Al <sub>2</sub> O <sub>3</sub>	13.8	13.73	13.4	13.9	13.8	14.1	14
Fe <sub>2</sub> O <sub>3</sub>	1.21	1.38	1.46	1.5	1.66	1.52	1.49
FeO	0.56	1.13	0.95	0.41	0.54	0.41	0.54
MnO	0.01	0.06	0.08	0.09	0.04	0.05	0.01
MgO	0.45	0.5	0.39	0.48	0.42	0.5	0.41
CaO	1.8	1.77	1.84	1.68	1.65	1.71	1.6
Na <sub>2</sub> O	4.3	4	3.96	4.2	4.1	4.1	4.2
K <sub>2</sub> O	3.65	3.8	3.7	3.8	3.45	3.7	3.7
P <sub>2</sub> O <sub>5</sub>	0.4	0.04	0.07	0.05	0.02	0.02	0.04
L.O.I	0.9	1.14	1.2	0.9	1.2	0.95	1.0
Total	99.88	99.95	99.9	99.73	100	99.96	99.17
<b>Trace elements (ppm)</b>							
Sr	35	43	55	33	52	47	40
Ga	17	19	22	23	25	20	18
Ba	550	448	466	530	441	370	487
Rb	88	92	78	99	83	107	95
Zr	270	255	310	283	199	218	257
Nb	35	33	31	28	37	42	38
Cr	4	3	5	4	2	9	10
Ni	2	1	1	1	2	4	3
V	4	5	7	3	2	4	4
Zn	43	48	52	43	55	44	32
Cu	7	8	3	3	2	2	4
Pb	17	15	13	11	18	17	14
Y	76	85	63	54	73	62	77

**Table 4: CIBW-norm and geochemical parameters of the investigated younger granites (monzogranites).**

Rock type	Monzogranites						
S. No.	M1	M2	M3	M4	M5	M6	M7
<b>CIPW normative minerals</b>							
Qz	30.57	30	31.56	29.56	31.91	30.36	30.44
Or	21.62	22.75	22.17	22.74	20.65	22.1	22.13
Ab	36.39	34.21	33.91	35.92	35.07	35	35.89
An	6.59	8.35	7.93	3.91	8.17	8.46	7.79
Di	-	0.24	0.72	0.18	-	-	-
Hy	1.13	1.37	0.76	1.13	1.06	1.26	1.04
Wo	-	-	-	-	-	-	-
Cor	0.35	-	-	-	0.32	0.62	0.21
MA	-	2.03	2.14	0.4	0.54	-	0.88
HM	1.21	-	-	1.24	1.31	1.54	0.9
ILM	1.21	0.96	0.67	0.81	0.88	0.98	0.6
Rut	0.07	-	-	-	-	0.14	-
Ap	0.87	0.09	0.15	0.11	0.04	0.04	0.09
<b>Geochemical parameters</b>							
C.I.	7.38	9.55	9.18	8.88	9.92	10.36	9.52
AGP.I.	0.8	0.78	0.79	0.79	0.74	0.71	0.76
D.I.	88.57	86.96	87.62	88.22	87.64	87.46	88.46
M.I.	79.73	83.39	86.07	79.92	83.97	79.42	83.2
F.I.	81.54	81.5	80.63	82.64	82.07	82.02	83.16

**Table 5: Chemical composition of the investigated younger granites (syenogranites)**

Rock type	Syenogranites								
S. No.	S1	S2	S3	S4	S5	S6	S7	S8	S9
<b>Major Oxides (wt. %)</b>									
SiO <sub>2</sub>	74.17	74	73.68	73.59	75.1	76	74.47	73.9	74.6
TiO <sub>2</sub>	0.3	0.24	0.3	0.4	0.3	0.5	0.4	0.47	0.48
Al <sub>2</sub> O <sub>3</sub>	13.1	13.0	13.4	13.3	13.0	12.85	13.1	13.3	13.2
Fe <sub>2</sub> O <sub>3</sub>	0.9	0.9	1.4	1.3	1.5	0.45	1.0	0.7	0.9
FeO	0.8	0.8	0.9	0.8	0.2	0.4	0.7	0.6	0.3
MnO	0.02	0.01	0.04	0.05	0.01	0.05	0.02	0.05	0.01
MgO	0.9	0.9	0.7	0.5	0.4	0.9	0.6	0.6	0.44
CaO	1.0	1.0	0.9	0.81	0.86	1.0	0.7	0.8	0.82
Na <sub>2</sub> O	4.2	4.3	3.6	4.3	3.6	3.9	4.0	4.2	4.0
K <sub>2</sub> O	3.0	3.6	4.1	3.8	3.4	3.6	4.18	4.1	4.18
P <sub>2</sub> O <sub>5</sub>	0.4	0.02	0.03	0.04	0.02	0.02	0.03	0.01	0.03
L.O.I	1.1	1.21	0.8	1.1	1.4	0.3	0.8	1.2	1.0
Total	99.89	99.98	99.85	99.99	99.79	99.97	100	99.93	99.96
<b>Trace elements (ppm)</b>									
Sr	23	25	21	17	15	18	27	19	22
Ga	31	26	31	26	28	25	29	27	32
Ba	62	57	47	50	52	44	53	60	48
Rb	211	232	237	217	222	242	210	235	240
Zr	300	288	295	342	350	299	277	320	333
Nb	46	50	53	44	55	41	55	52	43
Cr	3	4	6	7	8	12	10	13	11
Ni	1	3	3	2	1	1	2	4	3
V	3	2	2	3	1	1	1	2	2
Zn	67	58	49	57	55	63	66	47	56
Cu	4	3	2	4	5	3	3	2	1
Pb	18	23	17	22	25	26	19	21	20
Y	88	110	94	83	77	95	81	78	99

**Table 6: CIBW-norm and geochemical parameters of the investigated younger granites (syenogranites).**

Rock type	Syenogranites								
S. No.	S1	S2	S3	S4	S5	S6	S7	S8	S9
<b>CIPW normative minerals</b>									
Qz	36.13	32.04	34.47	32.04	39.42	36.25	33.18	31.62	33.37
Or	17.96	21.56	24.48	22.73	20.44	21.36	24.92	24.56	24.98
Ab	35.93	36.79	30.72	36.75	30.92	33.07	34.08	35.95	34.16
An	2.56	4.91	4.33	3.83	4.22	4.86	3.33	3.96	3.94
Di	-	-	-	-	-	-	-	-	-
Hy	2.55	2.63	1.84	1.26	1.02	2.26	1.51	1.52	1.11
Wo	-	-	-	-	1.9	-	-	-	-
Cor	2	0.24	1.47	0.72	-	0.75	0.78	0.51	0.66
MA	1.32	1.32	2.05	1.6	1.52	-	1.17	0.74	-
HM	-	-	-	0.21	0.45	0.45	0.2	0.2	0.91
ILM	0.58	0.46	0.58	0.77	0.95	0.95	0.77	0.9	0.66
Rut	-	-	-	-	-	-	-	-	0.14
Ap	0.88	0.04	0.07	0.09	0.04	0.04	0.07	0.02	0.07
<b>Geochemical parameters</b>									
C.I.	4.43	6.75	5.62	4.71	4.93	6.44	4.38	5.03	4.71
AGP.I.	0.78	0.84	0.77	0.84	0.74	0.8	0.85	0.85	0.84
D.I.	90.02	90.39	89.67	91.52	90.78	90.68	92.18	92.14	92.52
M.I.	65.38	65.38	76.67	80.77	80.95	48.57	73.91	68.42	73.17
F.I.	87.8	88.76	89.53	90.91	89.06	88.24	92.12	91.21	90.89

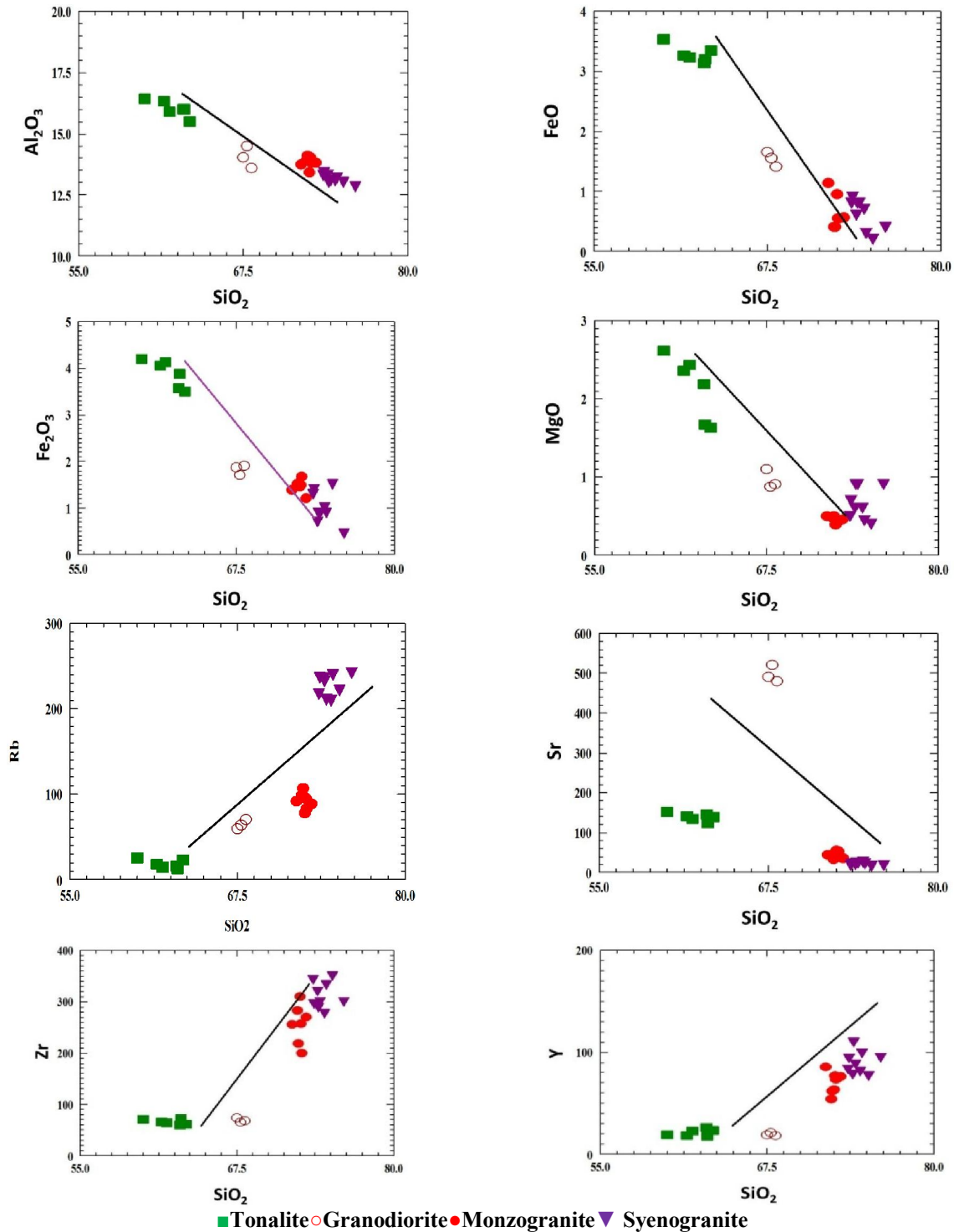


Fig. 6: Harker variation diagrams some of major oxides and trace elements against  $\text{SiO}_2$  for the granitic rocks of Rei El-Garrah area.

#### 4.2. Differentiation index versus major oxides and trace elements:

The plots of major oxides versus D.I. show that the  $\text{Al}_2\text{O}_3$ , FeO, CaO and MgO decrease with

increasing D.I. On the other hand, the plotting of some trace elements versus D.I. show that the Rb, Zr and Nb increase with increasing D.I. (Fig. 7).

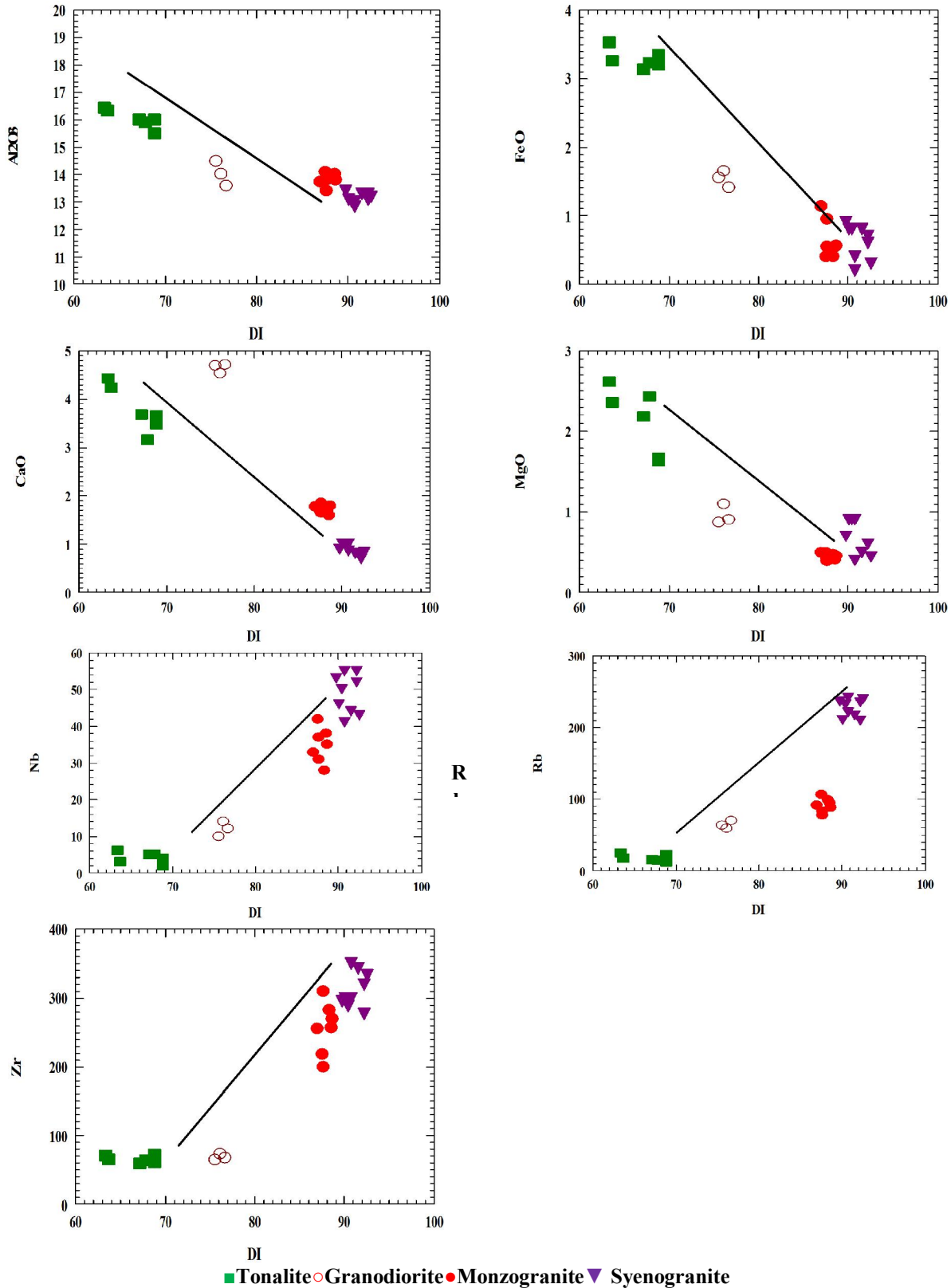
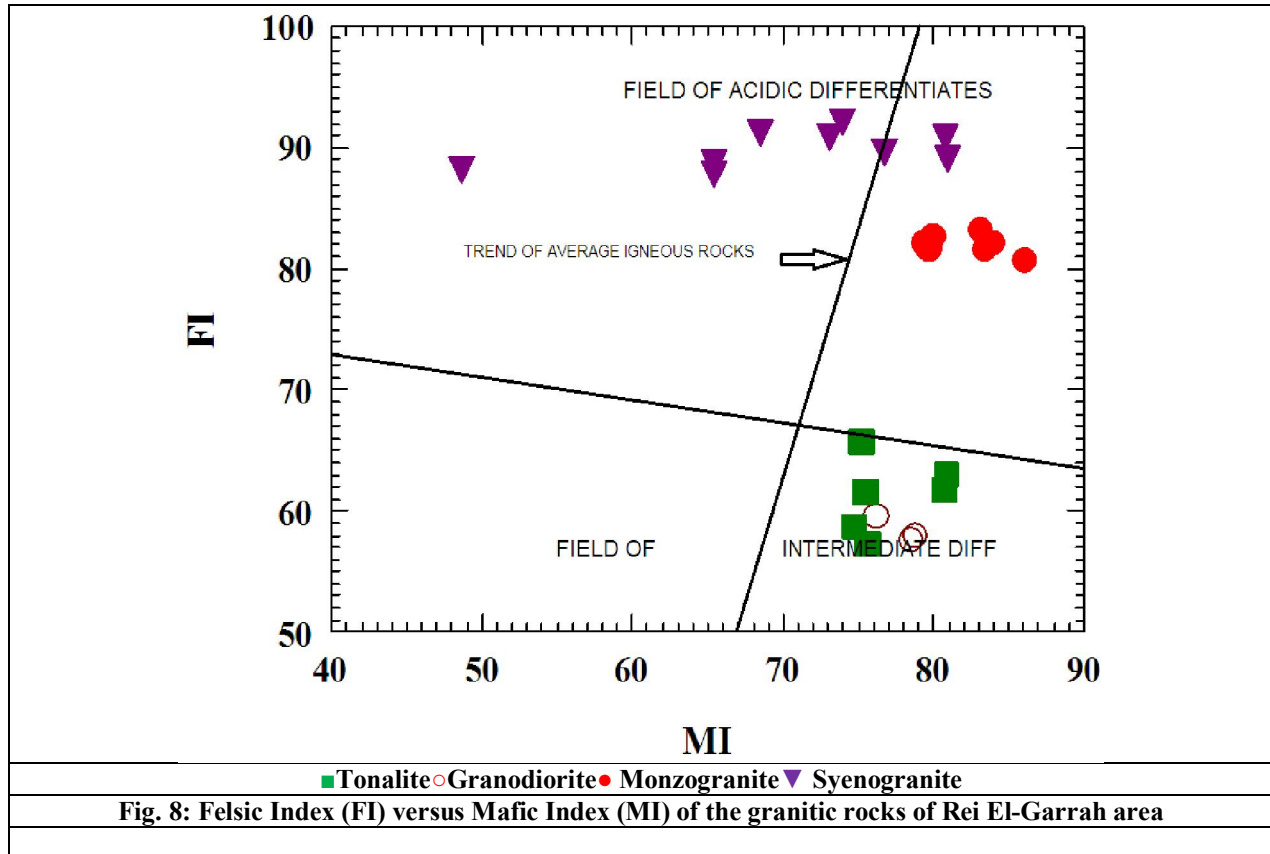


Fig. 7: Variation diagrams of some major oxides and trace elements against D.I. for the granitic rocks of Rei El-Garrah area

#### 4.3. Felsic and Mafic Indices

The relation between the felsic and mafic indices is shown in (Fig. 8). General trend of average igneous rocks suite of (Nockolds, 1954) is also shown. The data points of older granitoids (tonalite and

granodiorite) fall in the intermediate differentiation zone whereas those of the younger granites fall in the acidic and strong acidic differentiation zone with higher expected felsic indices.



#### a. CIPW normative values

The normative composition of the studied granitic rocks (Table 2, 4 and 6) shows that the granodiorite and tonalite have normative anorthite average contents 12.83 and 18.25% respectively whereas those of monzogranites and syenogranites are 7.31 and 3.99 % respectively. The normative average contents of albite in the monzogranites and syenogranites are 35.20 and 34.26 % respectively, whereas, the normative average contents of albite in the granodiorite and tonalite are 36.01 and 38.84%, respectively. The absence of normative corundum in granodiorite indicates metaluminous nature as will be shown later. On the other hand, the normative corundum in the younger granite samples are recorded in most samples of monzogranites and syenogranites, whereas normative diopside is absent in most samples of monzogranites and syenogranites. This reflects metaluminous to peraluminous nature of the studied younger granites.

#### 4.4. Geochemical classification and characterization

(Middlemost, 1985) proposed the SiO<sub>2</sub> versus (Na<sub>2</sub>O+K<sub>2</sub>O) variation diagram to classify the granitic rocks. This diagram shows that, tonalite samples plot in the tonalite field, granodiorite plot on the granodiorite fields and the younger granites plot in the granite field. The same results are given on Ab-Or-An ternary diagram of (O, Connor, 1965) that modified by (Barker, 1979), (Fig. 9.a & 9.b). On the normative Or-Ab-An ternary diagram of (Streckeisen, 1976), the older granitoids plot in the fields of tonalite and granodiorite whereas the younger granites plot in the fields of monzogranite and syenogranite (Fig. 9.c).

On the Rb-Sr-Ba ternary diagram proposed by (El-Bouseily and El-Sokkary, 1975), who classified the Egyptian granitic rocks into five fields. These fields are represented by quartz diorite, granodiorite, normal granite, highly differentiated granites and anomalous granite. According to this diagram, the tonalite and granodiorite samples plot in the tonalite

and quartz diorite field because of the close association of Sr and Ca. Monzogranites plot in normal granite because of high-Ba concentrations, which are typically associated with high-temperature K-feldspars in normal granites. Strontium shows more

or less uniform distribution in the normal granites group, while the increase in Ba is accompanied by a decrease in Rb. Syenogranites are mainly plotted in highly differentiated granites (Fig. 9.d).

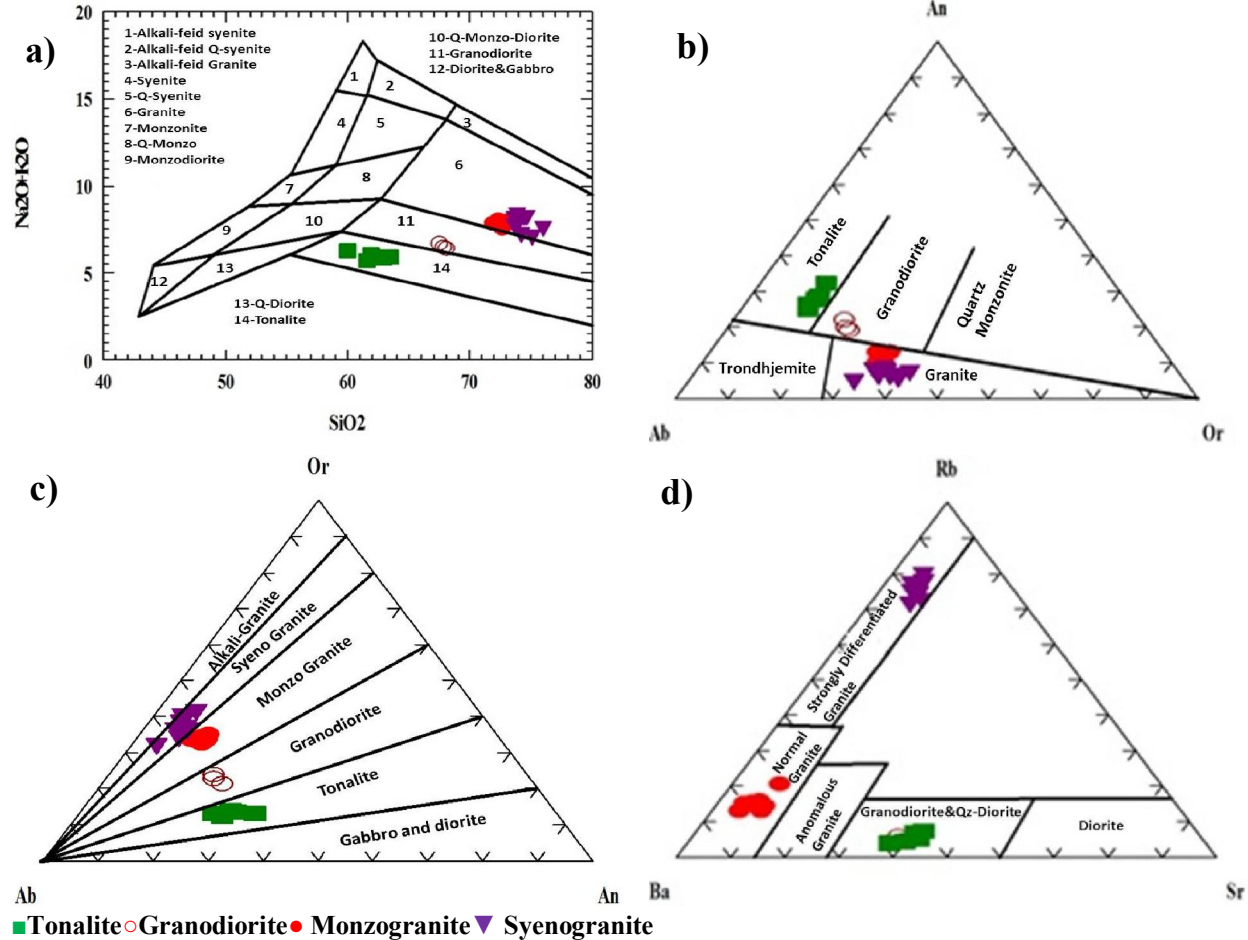


Fig. 9. a:  $\text{SiO}_2$  versus  $(\text{Na}_2\text{O}+\text{K}_2\text{O})$  variation diagram (Middlemost, 1985), for the granitic rocks of Rei El-Garrah area.

Fig. 9. b: Ab-Or-An ternary diagram (O'Connor, 1965 and modified by Barker, 1979) for the granitic rocks of Rei El-Garrah area.

Fig. 9. c: Ab-Or-An ternary diagram of Streckeisen (1976b) for the granitic rocks of Rei El-Garrah area.

Fig. 9. d: Rb-Ba-Sr ternary diagram of the granitic rocks (El-Bouseily and El-Sokkary, 1975) for Rei El-Garrah area.

#### 4.5. Magma type

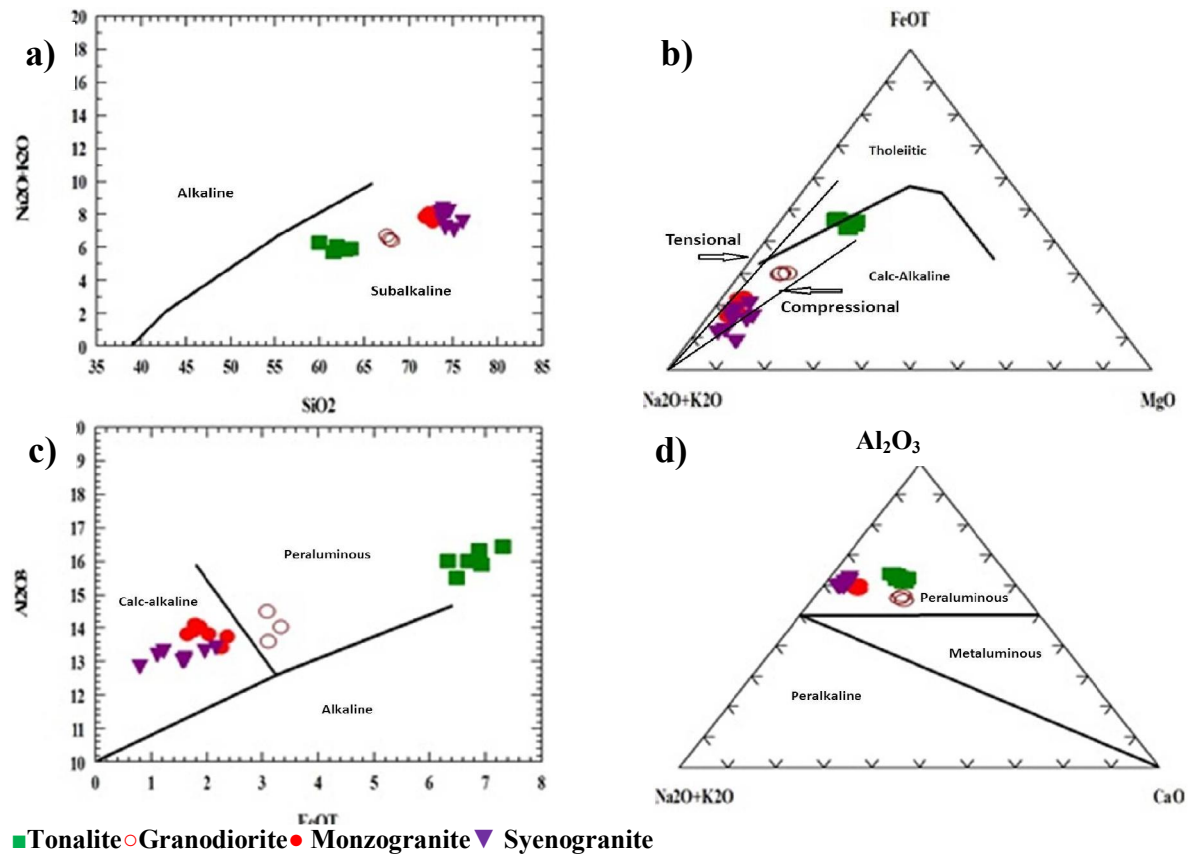
The AFM diagram,  $A=\text{Na}_2\text{O}+\text{K}_2\text{O}$ ,  $F=\text{Fe}_2\text{O}_3+\text{FeO}$  and  $M=\text{MgO}$  after (Irvine and Baragar, 1971) is used to differentiate between different magma types, the studied older granitoid samples lie toward AF side line and show calc-alkaline to slightly tholeiitic trend (Fig. 10. a), while the younger granites plot in calc-alkaline field due to the high total alkali contents and low MgO and  $\text{FeO}^t$  contents. This diagram was applied by (Petro et al., 1979) to discriminate between compressional and

extensional suites. The analyzed samples of the studied tonalite and granodiorites display mostly a trend of compressional suite. While the studied younger granite samples plot along the trend of extensional suite (Fig. 10. b).

Based on  $\text{FeO}^t$  versus  $\text{Al}_2\text{O}_3$  binary diagram suggested by (Abdel-Rahman, 1994) to distinguish between the alkaline, peraluminous and calc-alkaline magmatic nature. The studied older granitoids samples plot in the peraluminous field, while younger granite samples lie in calc-alkaline field (Fig. 10. c).

The alumina saturation ternary diagram (CaO)-(Na<sub>2</sub>O+K<sub>2</sub>O)-(Al<sub>2</sub>O<sub>3</sub>) of (Shand, 1951) is used to distinguish between the peraluminous, metaluminous

and peralkaline. All plotted samples fall in peraluminous field due to high contents of alumina (Fig. 10. d).



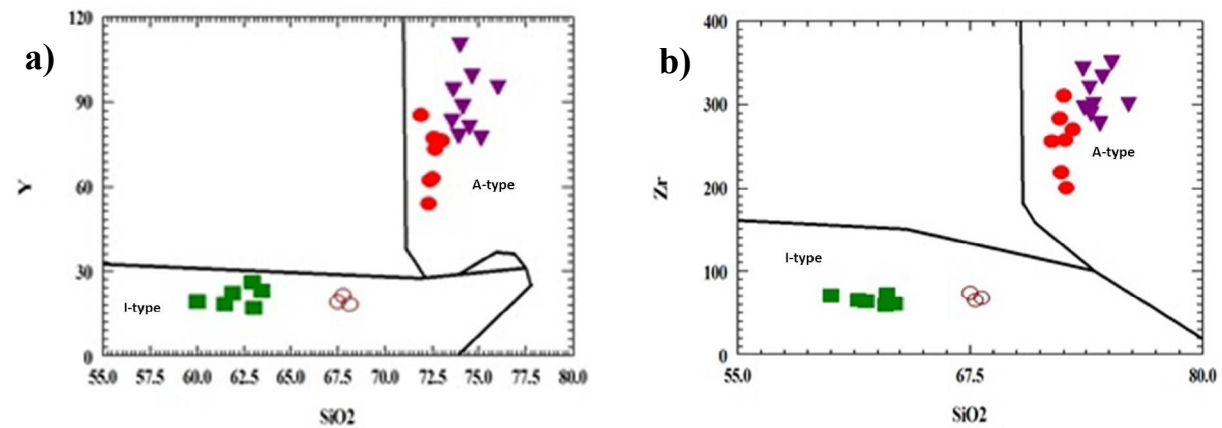
■ Tonalite ○ Granodiorite ● Monzogranite ▼ Syenogranite

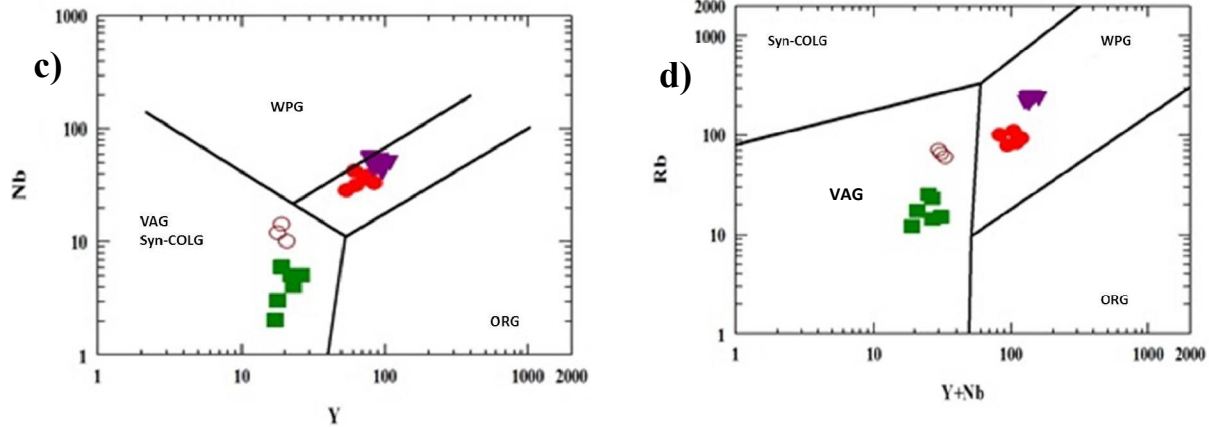
Fig. 10. a: TAS diagram of Irvine and Baragar, (1971) for the studied granitic rocks of Rei El-Garrah area.

Fig. 10. b: AFM diagram of Irvine and Baragar, (1971) modified by Petro et al., (1979) of the granitic rocks of Rei El-Garrah area.

Fig. 10. c: FeO<sup>t</sup>-Al<sub>2</sub>O<sub>3</sub> diagram of Abdel-Rahman, (1994) for the granitic rocks of Rei El-Garrah area.

Fig.10. d: CaO - ( Na<sub>2</sub>O + K<sub>2</sub>O ) - Al<sub>2</sub>O<sub>3</sub> discrimination diagram of Shand, (1951) for the granitic rocks of Rei El-Garrah area.





■ Tonalite ○ Granodiorite ● Monzogranite ▼ Syenogranite

Fig. 11. a:  $\text{SiO}_2$  versus Y binary diagram of Gunther et al., (1989) of the granitic rocks of Rei El-Garrah area

Fig. 11. b:  $\text{SiO}_2$  versus Zr binary diagram of Gunther et al., (1989) of the granitic rocks of Rei El-Garrah area

Fig. 11. c: Log Y versus Nb binary diagram of Pearce et al., (1984) of the granitic rocks of Rei El-Garrah area; VAG=Volcanic Arc Granites, Syn-COLG=Syn-collision granites, WPG=Within Plate Granites, ORG=Ocean Ridge Granites

Fig. 11. d: Log Rb versus (Y+Nb) binary diagram of Pearce et al., (1984) of the granitic rocks of Rei El-Garrah area; VAG=Volcanic Arc Granites, Syn-COLG=Syn-collision granites, WPG=Within Plate Granites, ORG=Ocean Ridge Granites

#### 4.6. Tectonic setting

$\text{SiO}_2$  versus Y and Zr binary diagrams of (Gunther et al., 1989) are used to differentiate between the different tectonic settings of the granitic rocks. All samples of older granitoids and are plotted on the I-type granites field. Meanwhile all samples of younger granites fall in A-type granites (Fig. 11. a & 11. b).

(Pearce et al., 1984) proposed the log Y-Nb and log Rb-(Y+Nb) binary diagrams to differentiate between the different tectonic settings of the granitic rocks. The older granitoids are plotted in the volcanic arc granite field, while the younger granites fall in the within plate granite field (Fig. 11. c & 11. d).

#### 4.7. Geochemical characteristics of the studied stream sediments:

Trace elements concentrations in the stream sediments result from the competing influences of provenance, weathering, diagenesis, sediment sorting and the aqueous geochemistry of the individual elements (Rollinson, 1993). Metals in stream sediments, soil and water have both geogenic (e.g., weathering of ultramafic rocks and phosphorite deposits, wind-blown dust,....etc.) and anthropogenic origins (e.g., urban development, extensive agriculture, industrial activities) (Alexakis, D., 2011; Batista et al., 2012; De Vos et al., 2006; Demetriades et al., 2010; Gamvroula et al., 2013; Papadopoulou-Vrynioti, 2002; Salminen et al., 2005 and Stamatis et al., 2011). In the present study, the collected forty one stream sediment samples were analyzed for trace

elements. The elements Cr, Ni, Cu, Zn, Zr, Rb, Y, Ba, Pb, Sr, Ga, V, and Nb were determined by XRF techniques. The obtained analytical data and some statistical parameters are given in (Tables 7 and 8).

The abundance of trace elements in Wadi El Missikat, W. Rei El Garrah, around W. Rei El Garrah, W. El Markh could be arranged according their abundance in the following order: Pb, Zr, Rb, Zn, Ba, Cu, Cr, V, Ga, Sr, Ni, Y and Nb, respectively (Fig. 12, 13 and 14).

It is clear that the studied stream sediments show extraordinary anomalous contents from Pb, Zr, Rb and Zn in correlation with the other trace elements (Table 7 and Fig.12). Wadi El Missikat contains the highest contents of Pb, Rb and Ga correlating to the other wadis which are mainly related to the presence of cotunnite ( $\text{PbCl}_2$ ) and other silicate minerals mainly originated from the surrounding granitic rocks. On the other hand, the area around Rei El Garrah contains the highest contents of Zr, Zn and Y in relation to other wadis resulting from the presence of zircon and other silicate minerals. However, Wadi El Markh has the highest contents of Cr, Ni, Zn and V with respect to other wadis which are mainly originated from the surrounding older granitoids and mafic-ultramafic rocks. (Table 9) presents the average contents of the trace element concentrations of the sediments of the study area with respect to average of soil concentrations obtained from other studies (Salminen et al., 2005; Vrynioti et al., 2013; Gromet et al., 1984; Ramadan et al., 2013; and El Nahas, 2006). (Table

9), together with (Fig. 13), while shows distinct inter-basin variation of element concentrations. The histograms for Pb display characteristically high values in the studied stream sediment samples due to the presence of cotunnite (PbCl<sub>2</sub>) in comparison with local and international samples but are lower than the corresponding values of European, G. Hamra and

South Quseir sediments in the other elements (see Table 9 and Fig. 13). Furthermore, for comparative purpose, the obtained data are normalized on the international shale standard namely; NASC (North American Shale Composite) which is given by (Gromet et al., 1984) and it was found that there is enrichment in Zr, Rb, and Pb (Fig. 14).

**Table. 7: Trace elements concentration (ppm) for stream sediments samples from the main Wadis of Rei El-Garrah area**

Wadis	S. No.	Cr	Ni	Cu	Zn	Zr	Rb	Y	Ba	Pb	Sr	Ga	V	Nb
W. El Missikat	1	40	24	76	73	296	92	23	116	2241	30	36	41	14
	5	29	21	71	74	159	103	12	78	1400	15	35	29	7
	19	33	17	65	90	143	155	11	62	933	13	37	23	6
	28	24	19	68	80	150	146	11	57	2583	12	10	19	7
	33	33	20	70	77	281	120	21	94	275	26	12	34	13
	35	36	21	85	85	345	143	26	95	1900	34	12	13	16
	37	33	21	52	88	328	131	25	91	3650	30	51	36	15
	38	43	27	68	94	403	132	30	117	1374	41	35	41	18
	40	42	28	77	94	202	132	15	81	2025	17	34	28	9
	53	52	35	76	84	282	66	22	145	1567	32	U,d	57	13
	55	42	22	74	90	179	110	13	93	1183	17	7	36	8
	56	21	15	68	78	182	193	14	45	1275	16	42	14	8
	57	31	18	70	70	206	115	15	78	1750	20	24	27	9
58	25	16	68	88	171	172	13	51	1533	13	14	18	7	
59	48	24	70	95	294	103	22	124	2233	28	U,d	44	13	
W. Rei El Garrah	42	32	17	71	82	186	104	14	79	2783	18	5	30	8
	66	35	25	72	93	244	143	19	76	2125	21	37	28	11
	67	31	16	71	71	217	134	16	69	1250	19	30	23	10
	73	34	24	67	74	304	105	23	100	1608	31	27	33	14
	74	24	16	69	77	115	157	9	41	1333	8	6	14	5
	77	32	22	85	53	98	60	8	75	1417	6	19	28	4
	78	32	22	65	93	287	120	22	92	1125	27	20	32	13
	79	30	17	71	108	225	96	17	111	1625	22	17	37	10
	84	32	20	56	97	289	123	22	87	3225	26	29	38	13
	94	13	15	70	109	207	114	16	85	700	17	36	29	9
95	32	24	70	81	308	97	23	93	1491	31	19	32	14	
Around Rei El Garrah	43	33	22	70	101	253	126	19	95	1542	23	26	30	12
	44	36	21	73	99	201	107	15	92	400	17	12	30	9
	48	36	24	72	87	293	99	22	96	780	29	7	33	13
	49	78	41	85	99	262	77	20	121	1767	24	4	63	12
	52	109	57	93	115	186	42	14	193	1892	16	27	122	8
	85	24	24	71	98	282	181	21	74	1508	26	11	22	13
	86	32	22	68	268	259	97	19	106	1100	24	45	34	12
90	45	27	79	103	263	71	20	122	8	27	21	42	12	
W. El Markh	54	78	50	77	81	216	49	16	154	2083	20	5	71	10
	61	79	43	77	89	193	106	15	172	425	16	34	80	9
	63	52	42	73	82	199	99	15	132	333	17	36	56	9
	64	51	38	74	81	228	87	17	143	708	22	15	59	10
	99	25	16	77	84	144	79	11	63	1058	13	23	22	6
	100	29	21	69	93	223	99	17	139	2417	21	32	65	10
	101	36	30	73	86	161	104	13	107	U,d	16	2	44	7

U,d = under limit of detection

**Table. 8: Minimum, maximum and average contents of trace elements concentration (ppm) for stream sediment samples from the main Wadis of Rei El-Garrah area**

Main Wadis	No.		Cr	Ni	Cu	Zn	Zr	Rb	Y	Ba	Pb	Sr	Ga	V	Nb
W. El Missikat	15	Min.	21	15	52	70	143	66	11	45	275	12	7	13	6
		Max.	52	35	85	95	403	193	30	145	3650	41	51	57	18
		Av.	35	22	71	84	241	128	18	89	1728	23	24	31	11
W. Rei El-Garrah	11	Min.	13	15	56	53	98	60	8	41	700	6	5	14	8
		Max.	34	25	85	109	308	143	23	111	3225	31	37	39	14
		Av.	30	20	70	85	225	114	17	83	1701	21	22	30	10
Around Rei El-Garrah	8	Min.	24	21	68	87	186	42	14	74	8	16	4	22	8
		Max.	109	57	93	268	293	126	22	193	1892	29	45	122	13
		Av.	49	30	76	121	250	92	19	112	1125	23	19	47	11
W. El Markh	7	Min.	25	16	69	81	144	49	11	63	333	13	2	22	6
		Max.	79	50	77	93	228	106	17	172	2417	22	36	80	10
		Av.	50	34	74	85	195	89	15	130	1004	18	21	57	9

No.= Number of samples; Min.=Minimum; Max.=Maximum and Av.= Average

**Table 9: Correlation between trace elements average of the studied stream sediments and other local and international averages.**

Averages	Cr	Ni	Cu	Zn	Zr	Rb	Y	Ba	Pb	Sr	Ga	V	Nb
1	41	26.5	72.8	93.8	227.8	105.8	17.3	103.5	1389.5	21.3	21.5	41.3	10.3
2	165.9	106.4	143.8	559	890.2	66.1	47.9	535.8	454.4	2076.8	10.36	50.3	7.1
3	25.7	15	66.5	44	66	165.8	227.5	70	241	21	186.2	12.5	22.2
4	92.9	35.3	22.1	120	-	-	-	-	38.6	171	-	68.3	-
5	124.5	58	-	200	125	35	636	-	142	-	130	-	13

- = not detected

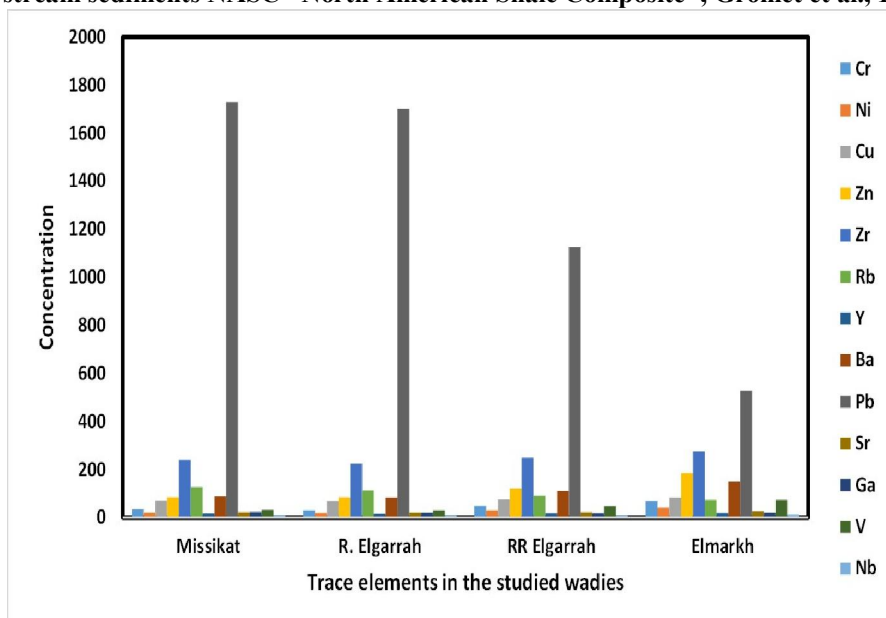
1= Average of stream sediments of Rei El-Garrah area (No. of samples = 41)

2= Average of stream sediments of South El-Quseir area (No. of samples = 25), Ramadan et al., 2013.

3= Average of stream sediments of Gabal Hamra area Southern Sinai (No. of samples = 43); El Nahas, 2006.

4= Average of stream sediments of European stream sediment samples (No. of samples = 852), Salminen et al., 2005 and Vrynioti et al., 2013.

5= Average of stream sediments NASC "North American Shale Composite", Gromet et al., 1984.

**Fig.12: Concentrations of trace elements in stream sediments from the main Wadis of Rei El -Garrah area.**

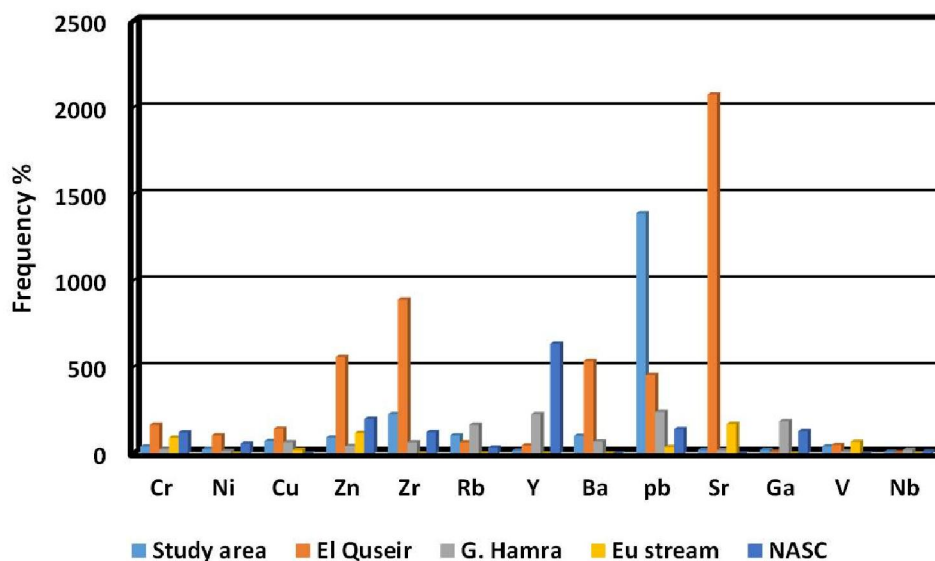


Fig. 13: Correlation between trace elements averages of the studied stream sediments and other local and international averages

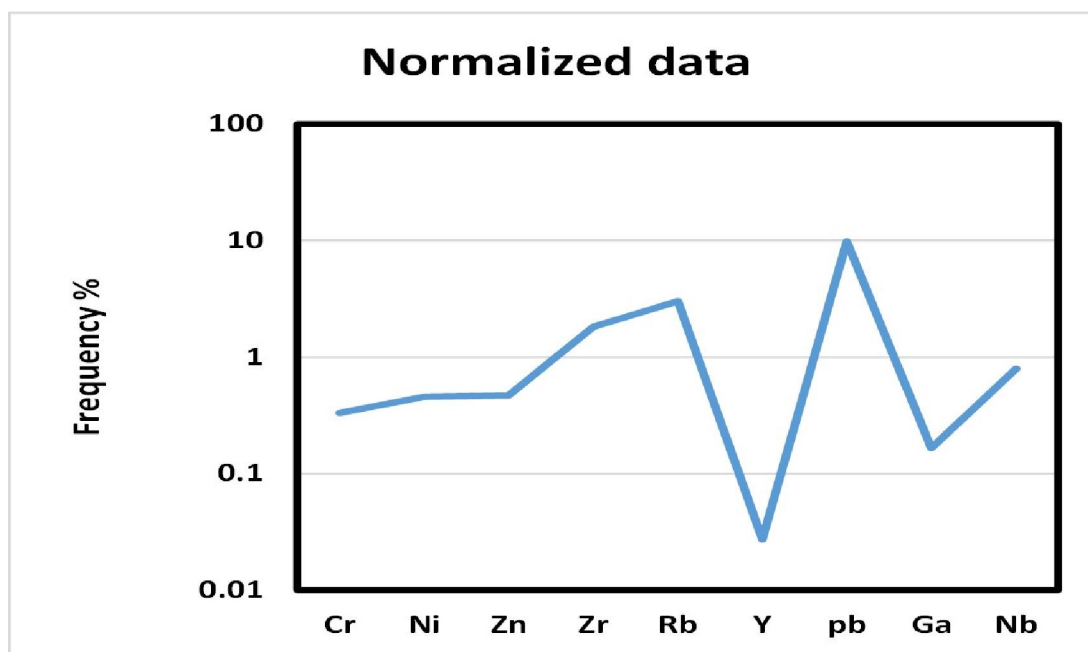


Fig. 14: Correlation between trace elements average of the studied stream sediments and NASC

### Conclusions

The study area is a part of the Central Eastern Desert of Egypt. It is bounded between latitudes  $26^{\circ} 23' 30''$  and  $26^{\circ} 31' 30''$  N and longitudes  $33^{\circ} 21' 30''$  and  $33^{\circ} 26' 40''$  E. The main exposures in the study area include comprise metavolcanics, older granitoids, younger gabbros, monzogranites, quartz-feldspar porphyry dykes and syenogranites. The main wadis are Wadi Rei El-Garrah, Wadi El-Missikat, Wadi El-Markh and Wadi El-Gidami. The older granitoids and younger granites are peraluminous due

to high alumina contents. They belong to a calc-alkaline suite with mild tholeiitic tendency evolved in a volcanic arc while the younger granites are calc-alkaline due to the high total alkali contents, low MgO and FeO<sup>t</sup> contents and originated in within-plate environment. The studied stream sediments show extraordinary anomalous contents from Pb, Zr, Rb and Zn in correlation with the other trace elements. Wadi El Missikat contains the highest contents of Pb, Rb and Ga correlating to the other wadis which are mainly related to the presence of cotunnite (PbCl<sub>2</sub>) and other silicate minerals mainly originated from the

surrounding granitic rocks. The area around Rei El Garrah contains the highest contents of Zr, Zn and Y in relation to other wadis resulting from the presence of zircon and other silicate minerals. However, Wadi El Markh has the highest contents of Cr, Ni, Zn and V with respect to other wadis which are mainly originated from the surrounding older granitoids and mafic-ultramafic rocks.

## References

1. Abdeen, M.M., Greiling, R.O., 2005: A Quantitative structural study of late pan-african compressional deformation in the central eastern desert (Egypt) during Gondwana assembly. *Gondwana Reserch* 8, 475-471.
2. Abdel-Rahman, A. F. M., 1994: Nature of biotites from alkaline, calc-alkaline and peraluminous magmas. *Journal of Petrology*, Vol. 35(2), pp. 525-541.
3. Alexakis, D., 2011: Diagnosis of stream sediment quality and assessment of toxic element contamination sources in East Attica, Greece. *Environmental Earth Sciences* 63 (6), 1369–1383.
4. Barker, F., 1979: Trondhjemite: Definition, environment and hypotheses of origin. In: F. Barker (ed). *Trondhjemite, Dacite and related rocks*. Elsevier, P.1-12. Barnes, H.L., ed., *Geochemistry of hydrothermal ore*.
5. Batista, M.J., Abreu, M.M., Locutura, J., De Oliveira, D., Matos, J.X., Silva, C., Bel-Lan, A., Martins, L., 2012: Evaluation of trace elements mobility from soils to sediments between the Iberian Pyrite Belt and the Atlantic Ocean. *Journal of Geochemical Exploration* 123, 61–68.
6. De Vos, W., Tarvainen, T., Salminen, R., Reeder, S., De Vivo, B., Demetriades, A., Pirc, S., Batista, M.J., Marsina, K., Ottesen, R.T., O'Connor, P.J., Bidovec, M., Lima, A., Siewers, U., Smith, B., Taylor, H., Shaw, R., Salpeteur, I., Gregorauskiene, V., Halamic, J., Slaninka, I., Lax, K., Gravesen, P., Birke, M., Breward, N., Ander, E.L., Jordan, G., Duris, M., Klein, P., Locutura, J., Bel-lan, A., Pasieczna, A., Lis, J., Mazreku, A., Gilucis, A., Heitzmann, P., Klaver, G., Petersell, V., 2006: *Geochemical Atlas of Europe. Part 2 — Interpretation of Geochemical Maps, Additional Tables, Figures, Maps and Related Publications*. Geological Survey of Finland, Espoo, Finland (<http://weppi.gtk.fi/publ/foregsatlas/> (Last accessed 1/6/2013)).
7. Demetriades, A., Li, X., Ramsey, M.H., Thornton, I., 2010: Chemical speciation and bioaccessibility of lead in surface soil and house dust, Lavrion urban area, Attiki, Hellas. *Environmental Geochemistry and Health* 32 (6), 529–552.
8. El Bouseily, A.M and El-Sokkary, A.A., 1975: The relationship between Rb, Sr and Ba in granitic rocks. *Chem. Geol.*, V.16, P174-189.
9. El Nahas, H.A. 2006: Distribution of nuclear minerals in G. Hamra Environs, Southern Sinai, Egypt. Ph.D. Thesis, Fac., Sci., Minufiya Univ., 159p.
10. El Ramly, M.F., 1972: A new geological map for the basement rocks in the Eastern and South-Western deserts of Egypt, scale 1:1,000,000. *Ann. Geol. Surv. Egypt* V. II, P.1-8.
11. El Reedy, M. W. (1984): The general physical and chemical features and the pollution level of El Sabahia-Sabhan-El Requa soil localities, State of Kuwait. Report represented to environmental protection Dept., Ministry of Public Health, El Kuwait (Part I: chemical methods).
12. El-Shazly, E. M., Bakhit, F. S. and Mostafa, M. E. 1981: Significant structure trends and the relation to radioactivity in El-Missikat granitic pluton, Central Eastern Desert, Egypt. *Proc. 6<sup>th</sup> Int. Cong. For Statis., Comp. Science, Social and Demogr. Research*, Ain Shams Univ., Cairo, pp. 399-418.
13. Gamvroula, D., Alexakis, D., Stamatis, G., 2013: Diagnosis of groundwater quality and assessment of contamination sources in the Megara basin (Attica, Greece). *Arabian Journal of Geosciences* 6 (7), 2367–2381.
14. Gromet, L.P., Dymek, R.F., Haskin, L.A., and Korotev, R.L., 1984: The “North American shale composite”—Its compilation, major and trace element characteristics: *Geochimica et Cosmochimica Acta*, v. 48, p. 2469–2482.
15. Gunther, J., Kleeman, M. and Twisted, D., 1989: The compositionally-zoned sheet-like granite pluton of the Bushveld complex: Evidence bearing on the nature of A Type magmatism. *J. Petrol.*, 30: 1383-1414.
16. Hietanen, A., 1963: Idaho batholith near Pierce and Bungalow. *U. S. Geol. Surv. P.* 344D.
17. Hussein, H. A. and El Kassas, J. A. 1980: Some favorable host rocks for uranium and thorium mineralization in Central Eastern Desert. *Ann. Geol. Surv. Egypt*, 10: 897-908.
18. Irvine, T. N. and Baragar, W.R.A., 1971: A guide to the chemical classification of the common volcanic rocks. *Can. Jour. Earth. Sc.* 8, 523-548p.
19. Middlemost, E.A.K., 1958: *Magma and magmatic rocks*. Longman group Ltd. London and New York, 75p.
20. Nockolds, S. R. 1954: Average chemical composition of some igneous rocks. *Geol. Soc. Amer. Bull.*, 62, 1007-1032.

21. O'Connor, J.T., 1965: A classification of quartz-rich igneous based on feldspar ratio. U.S. Geol. Surv. Prof. Paper No. 528 B.P. 79-84.
22. Papadopoulou-Vrynioti, K., 2002: Lost rivers associated with hazard pollution in Greece. Proceedings of 6th International Symposium on Speleology and Karstology AICaDi 55–61.
23. Pearce, J.A., Harris, N.B.W., Tindle, A.G., 1984: Trace element discrimination diagrams for the tectonic interpretation of granitic rocks. *J. Petrol.* 25, 956–983.
24. Petro, W.L.; Vogel, T.A. and Wilband, J.T., 1979: Major element chemistry of plutonic rock suites from compressional and extensional plate boundaries. *Chem. Geol.*, V.26, pp: 217-235.
25. Ramadan, F. S., El Balakssy, S. S. and Amer, O. T. 2013: Mineralogical and geochemical characteristics of the miocene-quaternary sedimentary FORMations, Wadi Wizr-Wadi Sharm El-Bahari Area, Central Eastern Desert, Egypt. *Jour. Sediment.*, pp.82.
26. Rollinson, H.R., 1993: *Using Geochemical Data: Evaluation, Presentation, Interpretation.* Longman (352pp).
27. Salminen, R., Batista, M.J., Bidovec, M., Demetriades, A., De Vivo, B., De Vos, W., Duris, M., Gilucis, A., Gregorauskiene, V., Halamic, J., Heitzmann, P., Lima, A., Jordan, G., Klaver, G., Klein, P., Lis, T., Locutura, J., Marsina, J., Mazreku, K., O'Connor, A., Olsson, P.J., Ottesen, S.Å., Petersell, R.T., Plant, V., Reeder, J.A., Salpeteur, S., Sandström, I., Siewers, H., Steenfelt, U., Tarvainen, A., 2005: *Geochemical Atlas of Europe. Part 1 — Background Information, Methodology and Maps.* Geological Survey of Finland, Espoo, Finland (<http://weppi.gtk.fi/publ/foregsatlas> (Last accessed 1/6/2013).
28. Shand, S.J., 1951: *Eruptive rocks.* John-Wiley, New York, 4<sup>th</sup> edition, 360p.
29. Shapiro, L and Brannock, W.W., 1962: Rapid analysis of silicate, carbonate and phosphate rocks, U.S. Geo. Surv. Bull. 114A P.1-56.
30. Stamatis, G., Alexakis, D., Gamvroula, D., Migiros, G., 2011: Groundwater quality assessment in Oropos–Kalamos basin, Attica, Greece. *Environmental Earth Sciences* 64 (4), 973–988.
31. Stern, R.J., Hedge, C.E., 1985: Geochronologic constraints on late Precambrian crustal evolution in the Eastern Desert of Egypt. *American Journal of Science* 285, 97-127.
32. Streckeisen, A.L., 1976a: Plutonic rocks: classification and nomenclature recommended by the IUGS subcommission on the systematic of igneous rocks, *Geotimes*, 18, 26-30.
33. Streckeisen, A.L., 1976b: Classification of the common igneous rocks by means of their chemical compositions. A provisional Attempt. *N. Jb. Min. Jour.*, 1-15.
34. Vrynioti K. P., Alexakis, D., Bathrellos, G. D., Skilodimou, H. D., Vryniotis, D., Vassiliades, E., Gamvroula, D. 2013: Distribution of trace elements in stream sediments of Arta plain (western Hellas): The influence of geomorphological parameters. *Journal of Geochemical Exploration*, 134, 17–26.

10/27/2017